Submitted to ApJ March 19, 2002
Preprint typeset using LaTeX style emulateapj v. 11/12/01

MICROLENS PARALLAXES OF BINARY LENSES MEASURED FROM A SATELLITE

David S. Graff and Andrew Gould
The Ohio State University Department of Astronomy, Columbus, OH 43210
graff,gould@astronomy.ohio-state.edu
Submitted to ApJ March 19, 2002

ABSTRACT

Caustic-crossing binary lenses make up about 5% of all detected microlenses. The relative proper motion of a caustic-crossing binary lens can be measured with observations from a single terrestrial telescope. Thus, uniquely, binary lenses can be completely solved with only the addition of a measurement of the microlensing parallax. This solution will yield the mass, distance, and transverse velocity of the lens relative to the source. To date, only one of the ~ 1000 observed microlensing events has been so solved.

We examine the ability of a parallax satellite combined with ground-based observations to solve these events. To measure both components of the vector parallax, the lens must be observed near two different caustics. Thus, the final accuracy is determined mostly by whether one can intensively monitor part of the first caustic crossing, by the magnification pattern, and by the path of the source with respect to the lens geometry. We find that vector parallaxes can be measured far more easily for binary lenses than single lenses, requiring 1-3 orders of magnitude fewer photons. They may thus yield a large number of completely solved lenses relatively cheaply.

Subject headings: gravitational lensing — stars:binaries — stars:mass function — Galaxy:bulge — Galaxy:stellar content

1. INTRODUCTION

In any microlensing event, there are four lens parameters of interest, its mass, M, the two components of its proper motion relative to the source, $\boldsymbol{\mu}_{\rm rel}$, and its parallax relative to the source, $\pi_{\rm rel}$. To measure these four parameters, one must measure four independent quantities. However, in standard microlensing, one measures only a single quantity of physical interest, the Einstein radius crossing time, $t_{\rm E}$. Thus, for the vast majority of microlensing events, one knows only a single degenerate combination of the four parameters, and can thus say very little about the lens. The individual parameters must be statistically inferred from a Galactic model. To date, the interpretation of microlensing results along every line of sight is subject to fierce controversy, as, in general, no standard Galactic model can explain any of the results. Fully solving microlensing events would allow us to measure the mass function of the Galactic bulge, study the spatial and kinematic structure of the Galaxy, and possibly determine the nature and location of at least a major component of Galactic dark matter.

The three other observable quantities that must be measured to solve an event are the angular Einstein radius, $\theta_{\rm E}$, the Einstein radius projected on the observer plane, $\tilde{r}_{\rm E}$ and the direction of the lens motion, α. All the lens parameters can be simply expressed in terms of these quantities (Gould 2000a). For example, the lens mass is given by

$$M = \frac{c^2}{4G}\theta_{\rm E}\tilde{r}_{\rm E}\,. \tag{1}$$

Of the roughly 1000 microlensing events observed to date, there are measurements of $\tilde{r}_{\rm E}$ for only about a dozen (Alcock et al. 1995; Bennett et al. 2001; Mao 1999; Soszyński et al. 2001; Smith et al. 2001; Bond et al. 2001; Mao et al. 2002; An et al. 2002), and measurements of $\theta_{\rm E}$ for a similar number (Alcock et al. 1997, 2000a, 2001a; Albrow et al. 1999a, 2000, 2001; Afonso et al. 2000; An et al. 2002). Typically, the events with measured $\tilde{r}_{\rm E}$ are the easiest few to measure, with longer than average time scales, and thus they do not characterize the lens population. Moreover, for only one of these (An et al. 2002) was it possible to measure both $\tilde{r}_{\rm E}$ and $\theta_{\rm E}$, and so to completely solve the event. To routinely solve typical microlensing events, and thereby measure M and other useful lens parameters, one must be able to routinely measure both $\tilde{r}_{\rm E}$ and $\theta_{\rm E}$. The projected Einstein radius $\tilde{r}_{\rm E}$ can be measured by comparing photometry of the event from the Earth and a satellite in solar orbit (Refsdal 1966; Gould 1994, 1995a). The angular Einstein radius $\theta_{\rm E}$ can be measured by tracking the excursion of the centroid of the lens images relative to the position of the source (Høg, Novikov & Polnarev 1995; Walker 1995; Miyamoto & Yoshi 1995). For typical events the scale of this excursion is only $\sim 100\,\mu$as, implying that only with space-based astrometric interferometers are accurate measurements feasible (Paczyński 1998; Boden, Shao & van Buren 1998).

All studies of astrometric mass measurements to date have considered only microlensing by single lenses, not binaries. At first this appears to be a very reasonable simplification because, while the majority of stars reside in binaries (Duquennoy & Mayor 1991), when the binary angular separation is much larger or smaller than $\theta_{\rm E}$, binary microlensing can hardly be distinguished from single-lens microlensing. Indeed, Alcock et al. (2000b) and Udalski et al. (2000) found that only $\sim 4-6.5\%$ respectively of observed events are caustic crossing binaries. A somewhat higher number are detected as binaries, but do not cross caustics, and a much larger number are undoubtedly binaries, but do not show significant deviation from a single lens lightcurve (Di Stephano 2000). To a first approximation, it therefore seems that not much is lost by ignoring this $4-6.5\%$.

In fact, this oversight is quite important. There are two key ways in which binary lenses are far easier to solve

than single lenses: they require many fewer photons to determine $\tilde{r}_{\rm E}$, and $\theta_{\rm E}$ can be determined without having to resort to astrometry.

First, we will show that for fixed source brightness, $\tilde{r}_{\rm E}$ can be determined for a binary microlens with only about 1% of the observing time required for single lenses. This means that $I = 17.5$ binary events can be measured in only one tenth the time needed for $I = 15$ single-lens events. And while $I = 15$ single-lens events are 15 times more frequent than $I = 15$ binary events, they have roughly the same frequency as $I = 17.5$ binary events. Hence, binary-lens events allow one to greatly increase the total number of measurements at a very modest observing cost.

Second, $\theta_{\rm E}$ can be independently measured from the ground in caustic-crossing binary lenses. This has been almost the only technique by which $\theta_{\rm E}$ has been measured to date [1]. The finite disk of the source star takes time $2\Delta t$ to cross the caustic, which can be measured directly from the lightcurve. This time is related to $\theta_{\rm E}$ by,

$$\frac{\Delta t}{t_{\rm E}}\cos\phi = \frac{\theta_*}{\theta_{\rm E}}\,, \tag{2}$$

where θ_* is the angular size of the source star, and ϕ is the angle of the source trajectory with respect to the normal to the caustic. The source star size, θ_* can be determined from its (dereddened) flux and effective temperature by

$$\mathcal{F} = \theta_*^2 \sigma T_{\rm eff}^4\,, \tag{3}$$

which relation has been best calibrated by van Belle (1999) using $(V-K)$ as a probe of surface temperature. Thus, if there is no high precision astrometry to determine $\theta_{\rm E}$, binary lenses will be essentially the only lenses that can be completely solved from parallax measurements.

2. THEORY

The Einstein angle of a binary lens is given by,

$$\theta_{\rm E}^2 = \frac{4G(M_1+M_2)}{Dc^2}, \qquad D \equiv \frac{D_{\rm ol}D_{\rm os}}{D_{\rm ls}}\,. \tag{4}$$

Here, $M_{1,2}$ are the lens masses, and $D_{\rm ls}$, $D_{\rm os}$, and $D_{\rm ol}$ are the distances between the observer, lens, and source. The projected Einstein radius,

$$\tilde{r}_{\rm E} = D\theta_{\rm E} \tag{5}$$

defines the scale of the magnification pattern projected onto the observer plane. The position of the observer in this plane in units of $\tilde{r}_{\rm E}$ is denoted $\boldsymbol{u}$.

Note that $\boldsymbol{u}\theta_{\rm E}$ is the angular displacement from the lens to the source as seen from an observer located at $\boldsymbol{u}\tilde{r}_{\rm E}$ in the observer plane. Thus, we caution the reader not to get confused that we will use $\boldsymbol{u}$ to refer both to the position of the source and the position of the observer. When discussing observations from a single telescope, which has characterized the situation in the vast majority of the microlensing literature, it is usually more convenient to think of a fixed observatory and a source moving behind the lens at location $\boldsymbol{u}\theta_{\rm E}$. When discussing simultaneous observations from several telescopes distributed about the solar system, it is more convenient to think of a group of telescopes moving through a fixed magnification pattern with individual telescopes located at $\boldsymbol{u}\tilde{r}_{\rm E}$. The two frames are perfectly consistent and interchangeable.

The photometric magnification is a function of $\boldsymbol{u}$, $A(\boldsymbol{u})$. The angular separation of the two elements of the lens is defined to be $\boldsymbol{d}\theta_{\rm E}$ with $\boldsymbol{d}$ pointing from the primary to the secondary. We will fix the origin of the $\boldsymbol{u}$ plane at the midpoint between the two stars in the binary. The two stars of the lens are thus located at $\pm\boldsymbol{d}/2$. It is conventional to align the coordinates of the $\boldsymbol{u}$ plane along $\boldsymbol{d}$.

The Sun moves through the observer plane with rectilinear motion:

$$\boldsymbol{u}_\odot(t) = \boldsymbol{u}_{0,\odot} + \boldsymbol{\mu}_\odot(t-t_0)\,. \tag{6}$$

while the other objects in the solar system are displaced from this position by their actual positions in the solar system projected along the line of sight, and brought into scale by dividing by $\tilde{r}_{\rm E}$. For example, the position of the Earth is

$$\boldsymbol{u}_\oplus = \boldsymbol{u}_\odot - \frac{\hat{\boldsymbol{n}}\times\hat{\boldsymbol{n}}\times\boldsymbol{a}_{\oplus\odot}(t)}{\tilde{r}_{\rm E}} \tag{7}$$

where $\hat{\boldsymbol{n}}$ is the unit vector in the direction of the source and $\boldsymbol{a}_{\oplus\odot}(t)$ is the displacement between the Earth and Sun. In this paper, we only consider observations over a short period of time, about 1 month. We will thus ignore the parallax effect of the Earth's motion around the Sun, and model the Earth's motion as rectilinear,

$$\boldsymbol{u}_\oplus(t) = \boldsymbol{u}_{0,\oplus} + \boldsymbol{\mu}_\oplus(t-t_0)\,. \tag{8}$$

We shall assume that there are two telescopes monitoring the event, say, one on the Earth and one on a satellite. The question before us is: how closely will one be able to determine the positions of the telescopes in the observer plane based on the magnifications recorded by the two telescopes? These two positions, that of Earth and the satellite, are related by

$$\boldsymbol{u}_\oplus - \boldsymbol{u}_s \equiv \delta\boldsymbol{u} = \frac{\hat{\boldsymbol{n}}\times\hat{\boldsymbol{n}}\times\boldsymbol{a}_{\oplus s}(t)}{\tilde{r}_{\rm E}}\,. \tag{9}$$

We see from equation (9) that $\tilde{r}_{\rm E}$ is inversely proportional to the observed quantity, $|\delta\boldsymbol{u}|$. It is therefore convenient to define the microlensing parallax $\pi_{\rm E} \equiv {\rm AU}/\tilde{r}_{\rm E}$.

Equation (9) relates two vectors, $\delta\boldsymbol{u}$ and $\hat{\boldsymbol{n}}\times\hat{\boldsymbol{n}}\times\boldsymbol{a}_{\oplus s}$. But these vectors are not a priori defined on the same coordinate axis. The rotation between these coordinate axes, α, is one of the unknown quantities that must be fit in a microlensing event. Effectively, one does not know a priori the direction of the projected Earth-satellite separation vector in the observer $\boldsymbol{u}\tilde{r}_{\rm E}$ plane, though one does know its length, $|\delta\boldsymbol{u}| = |\hat{\boldsymbol{n}}\times\hat{\boldsymbol{n}}\times\boldsymbol{a}|\pi_{\rm E}$. Therefore, we introduce the vector parallax $\boldsymbol{\pi}_{\rm E}$ as the quantity to be fit. We define $\boldsymbol{\pi}_{\rm E}$ to have length $\pi_{\rm E}$ and the same direction as the projected Earth-satellite separation. Thus, we have,

$$\delta\boldsymbol{u} = |\hat{\boldsymbol{n}}\times\hat{\boldsymbol{n}}\times\boldsymbol{a}_{\oplus s}|\boldsymbol{\pi}_{\rm E}\,. \tag{10}$$

Since $\boldsymbol{a}_{\oplus s}$ and $\hat{\boldsymbol{n}}$ are known, we can solve this equation for $\boldsymbol{\pi}_{\rm E}$. Measuring $\tilde{r}_{\rm E}$ is equivalent to measuring the positions of the Earth and the satellite in the observer plane, or more precisely, their difference, $\delta\boldsymbol{u}$.

Assuming that the lens is well modeled, i.e., that $A(\boldsymbol{u})$ is known, the accuracy in measuring the position of the

[1] The exceptions are MACHO 95-BLG-30 for which the source crossed the point caustic at the center of a single lens instead of the fold-caustic of a binary lens (Alcock et al. 1997), and MACHO LMC-5 for which $\theta_{\rm E}$ was measured with LMC astrometry (Alcock et al. 2001a).

observer depends on how rapidly the magnification varies with the position of the observer,

$$\frac{\sigma_{\rm phot}}{\sigma_u} \sim |\boldsymbol{\nabla} A(\boldsymbol{u})| \,. \tag{11}$$

That is, in a region where A is roughly constant, one learns little from a particular measurement, but in a region, such as the interior approach to a caustic, where A is changing rapidly, each measurement can strongly constrain $\boldsymbol{u}$. Note also that a single measurement can constrain only the component of $\delta\boldsymbol{u}$ in the direction of $\boldsymbol{\nabla} A$. At least two measurements are needed at different positions relative to the projected magnification pattern to fully determine $\tilde{r}_{\rm E}$.

For a single lens, there is only one region where $|\boldsymbol{\nabla} A|$ is large, near the point caustic at the center of the lens where $A \sim u^{-1}$ and thus $|\boldsymbol{\nabla} A| \sim u^{-2}$. By contrast, the binary lens has a network of caustics inside which $|\boldsymbol{\nabla} A| \sim \Delta u^{-1.5}$ and up to 10 cusps near which $|\boldsymbol{\nabla} A| \sim \Delta u^{-2}$. Here, Δu is the separation from the nearest caustic or cusp.

The caustics make a network of closed curves, enclosing regions in which there are five images of the source and separating them from the outer three-image region. Therefore caustic crossings always occur in pairs when the source passes into a caustic and then leaves it. In practice, events are not flagged as binary events until after the first caustic crossing, so intensive monitoring by a parallax satellite typically will not begin until then. In general, only the second caustic crossing will be intensively monitored, and thus can be used to strongly constrain $\pi_{\rm E\perp}$, the component of $\boldsymbol{\pi}_{\rm E}$ perpendicular to the second caustic crossing. Completely solving the lens requires $\pi_{\rm E\parallel}$, the component of parallax parallel to the second caustic crossing.

Near the second caustic crossing, the gradients of magnification are so steep that one can even determine $\pi_{\rm E\perp}$ using a terrestrial baseline of a few thousand km. Thus, it can be measured using two telescopes on Earth (Hardy & Walker 1995; Gould & Andronov 1999). As these authors discuss, three non-collinear telescopes on the Earth could completely determine $\boldsymbol{\pi}_{\rm E}$, but in practice, it is difficult to have two widely separated telescopes in the southern hemisphere able to monitor the second crossing, let alone three.

In this paper, we focus on the ability of a parallax satellite, with its much longer baseline, to determine $\pi_{\rm E\parallel}$. Such a measurement cannot be extracted from the second caustic crossing, and must come from other features in the magnification pattern. If the lens is observed near one of the other regions of high magnification, then $\pi_{\rm E\parallel}$ can be measured. For example, if the event is caught soon enough, while the magnification is still rapidly falling from the first caustic, the component of $\boldsymbol{\pi}_{\rm E}$ perpendicular to the first caustic crossing will be measured, which will in general not be parallel to the second caustic crossing. The full microlens parallax is also determined if the source passes near a cusp. There is also some weak constraint from the broader part of the magnification pattern not particularly near a caustic or cusp, where the gradient of magnification is gentle. The total influence of several such regions may make a significant contribution to $\pi_{\rm E\parallel}$.

We see therefore that the determination of $\tilde{r}_{\rm E}$, which requires measuring both components of $\boldsymbol{\pi}_{\rm E}$, will depend in a complicated fashion on the geometry of the lens and on the path of the source through that geometry. The range of events is thus best studied by Monte Carlo simulation.

3. SIMULATED EVENTS

3.1. *Ensemble of Microlensing Events*

We employ a Monte Carlo simulation to generate binary microlensing events roughly as they might be in real life. The goal here is not so much to create an accurate model of the Galaxy and of the event detection strategy, as to cover a variety of events. As the stellar density of the bulge follows a power law of $\rho \propto r^{-1.8}$, we have for simplicity drawn sources and lenses from a self-lensing isothermal sphere, which has the advantage that one can analytically solve for the distribution of source and lens distances (Gould 2000b). The lens relative velocity is drawn from a Maxwellian distribution with a two-dimensional velocity dispersion of $220\,{\rm km\,s^{-1}}$.

We choose the masses of both lenses in the binary from the "present day mass function" of Gould (2000b). This mass function has no high mass stars, but does include remnants such as white dwarfs and neutron stars appropriate to an old bulge population. Lacking further information about the distribution of binary-lens separations, we choose a flat distribution in $\log d$. Only a narrow region of lens separations, within a factor of two or so of $\theta_{\rm E}$, will create significant caustics, so our results should be relatively insensitive to the distribution of lens separations.

Once a lens is chosen, we randomly pick a path through the magnification pattern, jettisoning all events in which the path does not cross a caustic. This path is chosen with a uniform distribution in angular impact parameter $b\theta_{\rm E}$[2] We thus naturally weight towards lens separations with large caustics, that is, those with large $\theta_{\rm E}$, and for which the masses are separated by about $\theta_{\rm E}$, i.e., $|\boldsymbol{d}| \sim 1$.

We have assumed that observations will follow the trigger and follow-up model that has been profitably deployed to monitor binary lenses by several groups. A telescope, which may or may not be one of the two telescopes monitoring the event, finds the microlensing event when it starts to brighten. Once the survey telescope crosses a caustic, the event will be classified as a binary. This caustic crossing will trigger follow-up by the parallax telescopes, which we assume will begin observations 24 hours after the caustic crossing.

The time between caustic crossings (the amount of time that the observer spends in the 5-image region, hereafter the *caustic interior time* or $t_{\rm int}$) influences the ultimate accuracy of the measurement of $\boldsymbol{\pi}_{\rm E}$: if the caustic interior time is short, there will not be enough time to accurately measure the first caustic crossing and use it to measure $\pi_{\rm E\parallel}$. In Figure 1, we show the range of times between caustic crossings for both our model and those actually detected by the MACHO and OGLE experiments towards the Galactic bulge (Alcock et al. 2000b; Udalski et al. 2000).

We see that there is a poor match between the binary events generated by the model and those detected by the experiments: many more events with short caustic interior times are predicted than are actually detected. The

[2] In contrast to the usual technique for single lenses in which events are chosen from a uniform distribution in b, but are weighted towards large $\theta_{\rm E}$ events by multiplying the mass function by $m^{1/2}$.

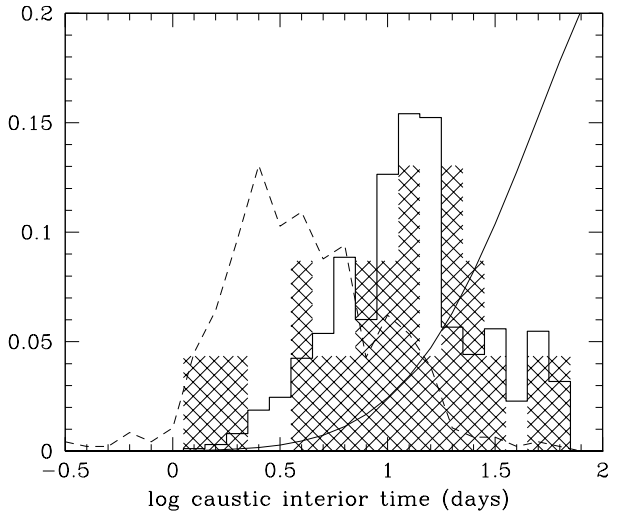

FIG. 1.— The dotted histogram shows caustic interior times $t_{\rm int}$ from our Monte Carlo model of binary caustic-caustic crossing microlensing events towards the Bulge. The shaded histogram shows $t_{\rm int}$ from the MACHO and OGLE collaborations. The smooth curve is the OGLE single-lens detection efficiency. The solid histogram is our Monte Carlo model weighted by the OGLE efficiency. Note that it better matches the observed binary lens events. From this figure, we see that most caustic-crossing binary events are missed because their caustics are too close together to have been detected by the surveys.

missing ingredient is a caustic-crossing binary detection efficiency. If caustic interior time is short, it is possible that this entire time will fall in a gap in the observations: there are often gaps of days due to weather and maintenance. Even if there are one or two points in the caustic, it might not be unambiguously classified as a caustic-crossing binary.

The caustic-crossing binary detection efficiency is difficult to calculate, since it should be calculated in a manner akin to the standard microlensing detection efficiency (e.g., Alcock et al. 2001b). It can only be calculated after the observations are complete and requires an extensive set of Monte Carlo experiments on the actual data. The efficiency will vary with the microlensing survey program. Such a calculation is well beyond the scope of this work.

Detecting a binary caustic-crossing event is akin to detecting a regular microlensing event: one needs to have a handful of observations across the event (or across the caustic interior portion of the binary event). We thus expect the caustic crossing binary detection efficiency as a function of $t_{\rm int}$ to be aproximately equal to the single lens detection efficiency for $t_{\rm E} \sim t_{\rm int}$. We show in Figure 1 how many caustic-crossing binary events are detected in our model assuming the OGLE efficiency of Udalski et al. (2000) can be applied to caustic-crossing binary events.

The predicted distribution is now in much better agreement with the actually detected binary events. The primary mismatch is the three detected events with short $t_{\rm int}$ which were all detected by the MACHO collaboration, and are not reproduced in the efficiency-modified model. One of these three events is a case for which the source passed in and out of the caustic interior twice, and would not have been well fit without the information from the other (long) caustic crossing. The other two are cases for which there was rapid high sampling frequency followup. These three cases could not be accounted for in the single star efficiency we adapted. The agreement between our efficiency-weighted model and the observed events (with the explained exceptions for short events) suggests that our model describes the actual caustic crossing binary events generated by the bulge.

3.2. *Dependence on observational strategy*

Since the two telescopes monitoring the event will likely be different, one terrestrial, and one satellite, we assume that one of the telescopes will have a far better signal-to-noise ratio (S/N) than the other. Our ability to measure $\boldsymbol{\pi}_{\rm E}$ will obviously scale linearly with the S/N of the weaker telescope.

If the satellite is the weaker telescope, then the photometric observations will likely be in the source-noise dominated regime, and the S/N will then scale as $N^{-1/2}$ where N is the total number of photons collected, depending in obvious ways on the magnitude of the source, size of the mirror, detection efficiency, pass-band, and exposure time. If the ground-based telescope is weaker, the source may be in the background-noise-limited regime, depending on the size of the seeing disk and the (magnified) brightness of the source compared to the bulge background of 18 mag arcsec^{-2}. We assume that the observations are in the source-noise regime, and we normalize our system to a total of 60,000 photons collected over all exposures[3] (ignoring magnification) or a total photometric S/N of 250.

From equation (10), the uncertainty in the microlens parallax $\boldsymbol{\pi}_{\rm E}$ is inversely proportional to the projected baseline, $|\hat{\boldsymbol{n}} \times \hat{\boldsymbol{n}} \times \boldsymbol{a}_{\oplus s}|$. We have chosen a nominal baseline $\boldsymbol{a}_{\oplus s}$ of 0.2 AU at a random orientation in the ecliptic, with the source direction $\hat{\boldsymbol{n}}$ in Baade's Window.

We assume that the parallax observations will not begin immediately after the first caustic crossing. Some time will be lost waiting for the next periodic observation, searching the data for a caustic-crossing event (which is presently reviewed by hand before announcing a trigger), communicating this alert to the microlensing community, and communicating new instructions to the parallax satellite. We have modeled this lost time as a 24 hour delay. This delay is potentially serious: the first caustic crossing may be missed. We determine the influence of this delay by simulating continuous observations with the delay set to 0 as well as to 24 hours.

The observational sampling rate can also be an important parameter. We probe two different sampling regimes: continuous sampling; and sparse sampling of once every 4 days, comparable to the typical time between caustic crossings $t_{\rm int}$ for bulge events. Note that the detected binary events shown in Figure 1 tend to have $t_{\rm int} > 4$ due to the low efficiency for short $t_{\rm int}$ events. These two regimes correspond respectively to what might be achieved

[3]To put this number into perspective, this corresponds to the number of photons recieved from an 18th magnitude source by the 0.9m CTIO telescope in 16 minutes of exposure.

by a network of terrestrial telescopes combined with a dedicated satellite, or what might be forced by a satellite that must be shared with other programs and with scheduling determined in advance.

We have made several simplifying assumptions. We have ignored the parallax effect of the Earth's circular motion around the Sun, approximating it as linear motion and we have ignored the slight difference in velocity between the satellite and the Earth. These give rise to small effects that are rigorously determined by the known motions of the Earth and satellite. Hence, they do not affect the error estimates relative to the naive analysis presented here.

3.3. *Analysis*

Fitting caustic-crossing binary microlensing events is still a difficult art (e.g., Albrow et al. 1999b). The sharp behavior of the caustics combined with a highly non-linear dependence on the lens parameters yield a complex χ^2 surface. Fortunately, we are not concerned in this paper with finding the best fit solution to a binary lens event, but with the precision of this solution once it is found.

In our simulation, information from the stronger telescope alone is used to fit all the parameters of a binary microlensing event that can be fit from a single telescope, d, q, ρ_*, $\theta_{\rm E}$, $\boldsymbol{u}_0$, $\dot{\boldsymbol{u}}$. Here, q is the mass ratio of the binary, and $\boldsymbol{u}_0$ is the location of the stronger telescope at some fiducial time t_0. There is no published study of the ability of a single telescope to measure these parameters for generic lenses, but experience on the few binary lenses that have been intensively followed to date shows that they can be fit very well. We will assume that observations from the stronger telescope can fit these parameters with essentially infinite precision, and we examine the ability of the weaker telescope to fit for the parallax.

Given a binary lens event with known parameters, we generate a time series of photometric measurements A_k, each with uncertainty σ_k. Using the Fisher matrix technique (e.g., Gould & Welch 1996), we determine the covariance matrix c_{ij} of the errors

$$c \equiv b^{-1}, \quad b_{ij} = \sum_k \sigma_k^{-2} \frac{\partial A_k}{\partial a_i} \frac{\partial A_k}{\partial a_i} \,. \tag{12}$$

Here the a_i are the various parameters being fit.

We fit for the following parameters: $a_i = \{\boldsymbol{\pi}_{\rm E}, F_s, F_b\}$. The blend flux, F_b, is unlensed light from a neighboring star. This light could be from a random interloper along the line of sight, a binary companion to the source, or from the lens itself. Due to blending, the measured flux is

$$F(\boldsymbol{u}) = F_s A(\boldsymbol{u}) + F_b \,. \tag{13}$$

The source flux F_s and the blend flux F_b must be independently determined at the weaker telescope except in the unlikely case that the two telescopes have identical band passes, air masses, and seeing conditions, which could only happen in practice if both telescopes were satellites.

3.4. *Results*

Our results are summarized in Figure 2, which shows the cumulative distributions of fractional errors, $(\sigma_{\tilde{r}_{\rm E}}/\tilde{r}_{\rm E})$ from Monte Carlo simulations of the four cases covering a variety of sampling strategies, and testing the effect of the caustic-crossing detection efficiency. We show continuous sampling beginning immediately after the first caustic crossing, continuous sampling beginning 24 hours after the first crossing, and sampling every four days (beginning $1-5$ days after the first caustic crossing) including and not including the caustic crossing detection efficiency.

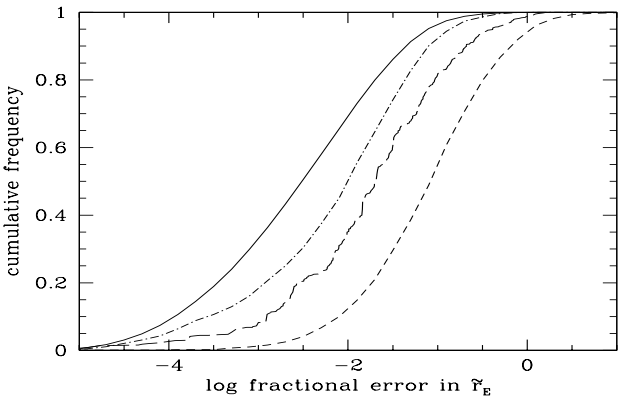

FIG. 2.— Cumulative distributions of the fractional error in $\tilde{r}_{\rm E}$ measured in a Monte Carlo sample of bulge caustic crossing binary microlensing events. From left to right, the curves are for (i) no delay before beginning continuous observations, (ii) 24 hour delay before beginning continuous observations, (iii) observations every 4 days, weighted by the caustic-crossing detection efficiency (iv) observations every 4 days with no weighting by efficiency. Efficiency weighting makes no difference in the continuous cases. The errors are normalized assuming a total of 60,000 photons (ignoring magnification) and a baseline of 0.2 AU.

These modes are listed in order of decreasing sampling agressiveness. Note from Figure 2 that curves representing these sampling strategies are arrayed from left to right: the most aggressive sampling strategies yield the highest accuracies even though the total telescope time is constant for these different realizations. The most aggressive strategy, continuous sampling beginning immediately after the first caustic, is about 30 times more sensitive than the least aggressive, sampling every four days beginning $1-5$ days after the first caustic.

Sampling strategy makes such a difference because there are a few small regions that best fix $\boldsymbol{\pi}_{\rm E}$: the areas immediately inside caustics and immediately around cusps have the highest magnification and strongest magnification gradients. By sampling at a high rate, we ensure that we catch the source while it is in these regions. Two such regions are needed to measure both components of $\boldsymbol{\pi}_{\rm E}$. The strategy of beginning observations immediately after the first caustic guarantees that both caustic crossings will be well covered.

The caustic interior time $t_{\rm int}$ has a strong effect on the fractional error in measuring the microlensing parallax. Events with a long $t_{\rm int}$ have lower fractional error in $\boldsymbol{\pi}_{\rm E}$ than events with short $t_{\rm int}$ as shown in Figure 3. Note from this figure that events with interior time $t_{\rm int} > 10$ days all have fractional error less than 0.1, while many of the shorter events have fractional error larger than 0.1. If the caustic interior time is short compared to the sampling

frequency or the delay from the first caustic crossing to the beginning parallax observations, it will be difficult to determine more than one component of $\boldsymbol{\pi}_{\rm E}$.

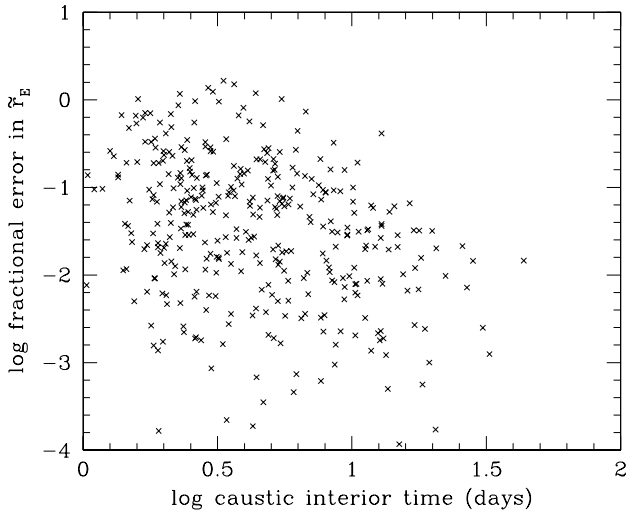

FIG. 3.— The fractional error in $\tilde{r}_{\rm E}$ plotted against the caustic interior time $t_{\rm int}$ (the time between the first and second caustic crossings). We have assumed sampling every four days. Note that events with $t_{\rm int} > 10$ days have much smaller errors than short events.

We test the effect of primarily including events with long $t_{\rm int}$ by including the caustic crossing detection efficiency for one of the curves in Figure 2. Reducing the short time events decreases the typical fractional error by about half a dex in the case of sampling every four days. It has little effect on the continuous sampling case. There is a small inconsistency here: if microlensing surveys are able to recognize potential binary events within 24 hours of the first crossing, they should have a higher sensitivity to short $t_{\rm int}$ events than we have modelled for the present day surveys. Such higher sensitivity can be achieved through aggressive groundbased followup of potential caustic crossing events. The MACHO collaboration pioneered such followup, leading to the excess of short $t_{\rm int}$ events in Figure 1.

4. DISCRETE DEGENERACIES

The Fisher matrix technique described above estimates the error in $\tilde{r}_{\rm E}$ once a solution is found. However, there may be more than one discrete solution to a set of observations, which could foil our ability to ultimately solve an event. The Fisher matrix technique is not suited to understanding the multiplicity of solutions, nor how serious these discrete degeneracies may be.

Parallax observations of a single lens suffer from a fourfold degeneracy. Observations with a single telescope fix the magnitude of that telescope's impact parameter, $|b|$. However, each telescope could pass on one of two sides of the lens (see Fig. 2 in Gould 1994). There are two physically distinct interpretations to any observation: either both telescopes pass on the same side of the lens, implying a large $\tilde{r}_{\rm E}$, or they pass on opposite sides of the lens, implying a small $\tilde{r}_{\rm E}$.

Fortunately, this symmetry is broken for binary lenses (except in the special case for which the lens motion $\boldsymbol{\mu}$ is parallel to the binary axis $\boldsymbol{d}$). Paths on opposite sides of the center of the lens will generate different lightcurves. However, binary lenses can suffer from other degeneracies. Moderately sampled lenses can be fit by several models (Dominik 1999a), and even extremely well sampled events can suffer from the wide-close degeneracy (Dominik 1999b). When the binary separation is wide compared to $\theta_{\rm E}$, the caustic breaks up into two four-cusped caustics. In a close binary, the caustic breaks up into three caustics, two with three cusps and one with four cusps. In cases for which the binary is very wide or very close, for a given lightcurve passing close to or through a four-cusped caustic, there will be two solutions, one through the four-cusped central caustic of a close binary, and one through a four-cusped caustic from a wide binary.

For example, event MACHO 98-SMC-1 (Afonso et al. 2000), a binary microlens in the Small Magellanic Cloud, is one of the best observed microlensing events. It was followed intensively by every microlensing group, including observations every 5 minutes over the second caustic with 1% precision. Despite these excellent data, there remain two solutions, a wide solution and a close solution.

This degeneracy means only that the magnifications $A(\boldsymbol{u})$ are similar along the particular path of the stronger telescope through the magnification pattern. The weaker telescope probes a separate path through this pattern, parallel to, but offset from the path of the stronger telescope. The criterion for breaking the degeneracy is that only one of the two possible solutions, wide or close, should be able to fit the lightcurve of the weaker telescope.

We simulate the wide-close degeneracy of event MACHO 98-SMC-1 to determine if a parallax telescope would break the degeneracy. Assuming that the event really was the wide solution of Afonso et al. (2000), we generate mock data from a parallax satellite offset by $\boldsymbol{\delta u}_w$ from the wide solution. We then search parallax offsets $\delta\boldsymbol{u}_c$ from the close binary solution to find the one that best fits the lightcurve from the parallax satellite in the wide solution. Two such solutions are shown in Figure 4. We find that the difference between the two parallax satellite light curves is small, comparable to the difference between the two solutions from the ground. Thus, photometry from a parallax satellite will not break the degeneracy.

In MACHO 98-SMC-1, the caustics do not have the same shape, though in more extreme cases such as MACHO 99-BLG-47 (Albrow et al. 2002) the caustics almost coincide. When the caustics from the two solutions do not coincide, it is possible to break the degeneracy if the photometric observations are combined with astrometric observations. Photometric observations of any binary microlensing event, combined with a model of the lens, determine the orientation of the lens in solar-system coordinates: the separations $\delta\boldsymbol{u}$ (in the lens frame) is parallel to the separation between the two telescopes projected along the line of sight (in the solar system frame), as described by equation (9). The angle α between the motion of the magnification pattern through the solar system and the projected Earth-satellite baseline is equal to the angle be-

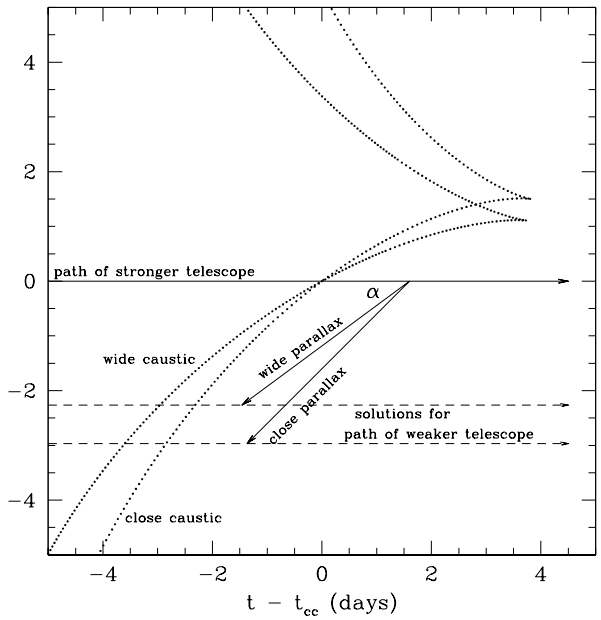

FIG. 4.— Caustics from the two solutions to degenerate event MACHO 98-SMC-1 have been rotated and scaled so that the path of the earth during that event lies on the x axis. The units are days from the second caustic crossing. Also shown are two possible degenerate solutions to photometry from a parallax satellite. However, the two solutions could possibly be distinguished if the angle α were independently measured astrometrically.

tween $\delta\boldsymbol{u}$ and the source motion,$\boldsymbol{\mu}$ (see Figure 4).

If the caustics for the two solutions do not coincide, then $\delta\boldsymbol{u}$ will be different for the two solutions. For example, it is possible that both telescopes will see the second caustic crossing at the same time. In that case, $\delta\boldsymbol{u}$ is parallel to the caustic. But since the caustics in the two models do not cross the source trajectory at the same angle, the angle between the source trajectory and the baseline will differ between the two models. Note that the two parallaxes in Figure 4 are different, and most important, have different values of α.

However, as discussed by Gould & Han (2000), the motion of the centroid of light in the vicinity of the caustic is also degenerate: it is similar for both the wide and close solutions. Thus, astrometric observations will generate the same value of α for both the wide and close solutions, while as discussed above, the photmetric parallax measurements will determine two different values of α depending on the solution. Only one of these solutions will match both the parallax and astrometric determinations of α.

Gould & Han (2000) showed that away from the caustic, the long-term behavior of the motion of the image centroid is different for the two solutions and can thus break the degeneracy. The advantage of our technique of comparing the direction of the source motion determined both from parallax and from astrometry is that it relies only on the astrometric observations of the caustic-crossing portion of the event, when the event is far brighter than at baseline, allowing a great saving in astrometric observing time.

There has, to date, been no systematic study of the wide-close degeneracy. We understand why it occurs in the limit of extreme-wide and extreme close binaries (Dominik 1999b). However, we do not know how wide or close a binary must be before it is susceptible to this degeneracy. Thus, we cannot tell how many of the binary events will suffer from this degeneracy.

5. POSSIBLE FUTURE MISSIONS

SIM, the *Space Interferometry Mission* (SIM)[4] is an interferometric astrometric satellite with two effectively 25 cm mirrors, separated by a baseline of 10 m. One of the key projects of SIM is to follow microlensing events; only SIM can *routinely* measure $\theta_{\rm E}$ for single lens microlens events, which it does by measuring the motion of the centroid of the image of the source star (Boden, Shao & van Buren 1998; Paczyński 1998). SIM will also measure $\tilde{r}_{\rm E}$ for these events using the same technique proposed in this paper for measuring $\tilde{r}_{\rm E}$ in binary lenses (Gould & Salim 1999).

SIM is at present expected to be in a trailing solar orbit, moving away from the Earth at 0.1 AU/yr. For present purposes, we have put SIM at 0.2 AU. SIM will observe bulge microlensing events in a predetermined schedule every 4 days, and is thus our archetype of a sparse-sampling satellite. Microlensing events will be discovered by a ground-based survey telescope. Then, after a binary event crosses the first caustic, SIM could begin monitoring this event every 4 days.

Our normalization corresponds to 1 hour of SIM observations on an $I = 18$ source. In comparison, when studying single lenses, Gould & Salim (1999) assumed an $I = 15$ source with 5 hours of observations, 80 times the number of photons that we have assumed here. The typical errors they determined for single lenses, a few percent, are comparable to those we find here for binary lenses, but the single lens requires two orders of magnitude more photons.

As SIM is primarily an astrometric and not a photometric mission, it will also monitor the image centroid motion of the microlensing event. This motion can be used to determine $\theta_{\rm E}$ in single lens events and non-caustic-crossing binary lens events, though it is not needed for this purpose in caustic-crossing binaries since $\theta_{\rm E}$ can be determined from the lightcurve alone.

Parallaxes do not have to be measured with SIM; many other satellites could serve as well. Consider a satellite like the GEST satellite[5], but located at L2 (GEST is proposed to be in polar Earth orbit). With its 2m telescope, GEST would have a photometric $S/N \sim 6$ times that of SIM (for the same exposure time) while the baseline with respect to the Earth would be ~ 10 times smaller than SIM in its Earth trailing orbit. Thus, GEST would be able to measure parallaxes with comparable precision to SIM given the same total exposure time. However, GEST is proposed to continuously image ~ 6 fields in the bulge, so its total exposure time would be ~ 6 days for a microlensing event, 144 times the 1 hour that we have assumed for SIM. Thus, GEST could measure parallaxes with about an order of magnitude greater accuracy than SIM could if SIM were sampling continuously, which is another order of magnitude better on average than SIM with sampling every 4 days.

[4] http://sim.jpl.nasa.gov

[5] http://bustard.phys.nd.edu/GEST

GEST photometry would be so strong, with continuous sampling before as well as during the event, that the ground based telescope would serve as the weaker follow up telescope, the converse of the SIM case. Still, given proper follow-up, much higher accuracies in measuring $\tilde{r}_{\rm E}$ could be achieved than in the SIM example discussed above.

6. DISCUSSION

For the SIM example, our results are broadly comparable to the accuracies derived by Gould & Salim (1999). But those authors assumed a 15th magnitude source with 5 hours of exposure time, 80 times as many photons as we assumed here for binary lenses. In effect, caustic crossing binary lenses are almost two orders of magnitude more efficient than single lenses, and three orders of magnitude more efficient with rapid sampling. The number of lenses studied by SIM could be greatly increased with only a minor cost in observing time.

Since binary lenses are so much easier to study than single lenses, many binary stellar masses could be harvested by SIM. But are these masses scientifically useful? After all, SIM will measure at least 200 masses of binary stars with 1% precision through standard techniques.

However, standard techniques can only be applied to nearby binaries with at least one luminous component. Only microlensing can measure the masses of stars in the bulge, and the masses of dark binaries [though the masses of neutron stars and their (possibly dark) companions can be measured in a few cases using relativistic effects and pulsar timing (Thorsett & Chakrabarty 1999)]. Further, the binary masses identified through a microlensing program will have a completely different selection function than those observed through standard techniques.

As we have seen, the uncertainty in a microlensing mass measurement depends on whether or not the source crosses a caustic. Some binary lenses have broader caustic networks than others, with a greater chance of crossing a pair of caustics sufficiently widely spaced to allow an accurate parallax measurement. For any set of lens parameters $\{b, q, \theta_{\rm E}, \tilde{r}_{\rm E}, t_0\}$ that will be determined from ground-based observations, we can define the *efficiency of detection* to be the fraction of paths that allow a mass measurement of a desired accuracy. This efficiency may be a complicated function of the lens parameters, but it can be determined using Monte Carlo techniques (e.g., Alcock et al. 2001b).

We thank Scott Gaudi for many useful discussions. This research was supported by JPL contract 1226901.

REFERENCES

Afonso, C., et al. 2000, ApJ, 532, 340
Albrow, M. D. et al. 1999a, ApJ, 522, 1011
——-, ApJ, 522, 1022
——- 2000, ApJ, 534, 894
——- 2001, ApJ, 549, 759
——- 2002, ApJ, submitted, astro-ph/0201256
Alcock, C., et al. 1995, ApJ, 454, L125
——- 1997, ApJ, 491, 436
——- 2000a, ApJ, 534, 894
——- 2000b, ApJ, 541, 270
Alcock, C. et al. 2001a, Nature, 414, 617
——- 2001b, ApJS, 136, 439
An, J. et al. 2002, ApJ, in press, (astro-ph/0110095)
Bennett, D. P., et al. 2001, ApJ, submitted (astro-ph/0109467)
Boden, A. F., Shao, M. & van Buren, D. 1998, ApJ, 502, 538
Bond, I. A. et al. 2001, MNRAS, 327, 868
Di Stephano, R. 2000, ApJ, 541, 587
Dominik, M. 1999a, A&A, 341,943
Dominik, M. 1999b, A&A, 349, 108
Duquennoy, A., & Mayor, M. 1991, A&A, 248, 485
Gould, A. 1994, ApJ, 421, 72
——- 1995a, ApJ, 441, 21
——- 1995b, ApJ, 446, 71
——- 2000a, ApJ, 542, 785
——- 2000b, ApJ, 535, 928
Gould, A. & Andronov, N. 1999, ApJ, 516, 236
Gould, A. & Han, C. 2000, ApJ, 538, 653
Gould, A. & Salim, S. 1999, ApJ, 524, 794
Gould, A. & Welch, D. 1996, ApJ, 464, 212
Hardy,S.J. & Walker, M.A. 1995, MNRAS, 276, L79
Høg, E., Novikov, I. D., & Polnarev, A. G. 1995, A&A, 294, 287
Mao, S. 1999, A&A, 350, L19
Mao, S., et al. 2002, MNRAS, 329, 349
Miyamoto, M., & Yoshii, Y. 1995, AJ, 110, 1427
Paczyński, B. 1998, ApJ, 494, L23
Refsdal 1966, MNRAS, 134, 315
Smith, M. C., Mao, S., & Woźniak 2001, MNRAS, submitted (astro-ph/0108214)
Soszyński, I., et al. 2001, ApJ, 552, 731
Thorsett, S.E. & Chakrabarty, D. 1999, ApJ, 512, 288
Udalski, A., Zebrun, K., Szymański, M., Kubiak, M., Pietrzyński, G., Soszyński, I., & Wozniak, P. 2000, Acta Astronomica, 50, 1
van Belle, G.T. 1999, PASP, 111, 1515
Walker, M. A. 1995, ApJ, 453, 37